Tunneling Induced Electroluminescence from Metal-Oxide-Semiconductor Structure on Silicon

*Ching-Fuh Lin [*a], Cheewee Liu, Miin-Jang Chen [a], Ming-Hung Lee, and I-Cheng Lin

Department of Electrical Engineering, National Taiwan University, Taipei, Taiwan, ROC

[a] also with Graduate Institute of Electro-Optical Engineering

ABSTRACT

Silicon is the most important semiconductor material for electronics industry. However, its indirect bandgap makes it hardly emit light, so its applications in optoelectronics are limited. Many efforts had been devoted to converting silicon to light-emitting materials, including porous silicon-based devices, nanocrystalline Si, and so on. In this work, we report electroluminescence on silicon with simple metal-oxide-semiconductor (MOS) structure. The thin oxide is grown by well-controlled rapid thermal oxidation. With extremely thin oxide, significant tunneling current flows through the MOS structure as the metal is properly biased. The tunneled electrons could then occupy the upper energy levels more than the thermal-equilibrium situation. Then luminescence occurs when they have radiative transition to lower energy states. For low biased voltages, the emission occurs around 1150 nm, approximately corresponding to the Si bandgap energy. For large applied voltages, the emission shifts to longer wavelengths and becomes voltage-dependent. MOS structures fabricated on both p-type and n-type silicon exhibit electroluminescence. This is significant because the fabrication of those MOS structures is compatible with CMOS electronics. Therefore, the MOS EL devices provide a particular advantage over other types of luminescence on silicon. The details of the electroluminescence and its physical reason are reported and discussed.

Keywords: Electroluminescence, silicon, metal-oxide-semiconductor, CMOS, rapid thermal oxidation, radiative transition, tunneling current.

1. INTRODUCTION

The mature technology of Si had made it the most important material for integrated-circuit (IC) industry. The popularity and low-cost Si technology had caused IC industry to penetrate many aspects of human life after 1950s. Therefore, many efforts had also been devoted to making Si useful for optics and optoelectronics, hoping to extend Si technology to more areas. There had been some achievements in the applications of Si processing technology to the fabrication of optoelectronic components. They include detectors, waveguides, [1] modulators, [2] wavelength demultiplexers, [3] and micro-optics. [4] Even with those components, integration of optoelectronics into Si-based technology is still limited because light emission directly from Si material is not feasible. The main obstacle is due to the indirect-bandgap nature, which causes light emission from Si to be extremely challenging.

1.1. Review of Luminescence from Silicon

Many groups had searched ways to overcome this obstacle. Those efforts include porous-silicon-based devices, [5-7] doping impurity into Si, [8-10] Si^+-implanted SiO_2, [11, 12] alloying Si with Ge or Sn, [13, 14] nanocrystalline Si, [15, 16] or quantum-confinement structures, [17] deposition of polymer on Si substrates, [18] growth of GaN on Si substrates, [19, 20] and so on. Porous Si mostly emits visible light. Its physics of luminescence had been attributed to surface states, surface species, and quantum confinement. [21] The exact mechanisms are still not well known. Doping impurities into Si utilizes luminescence centers like Er^{3+} or other ions. The low solid solubility and small interaction cross section are serious hurdles for such applications. Alloying Si with Ge or Sn and nanocrystalline Si are based on the theory and engineering of band structures, trying to modify the indirect-bandgap nature of Si to direct bandgap. Its success very depends on the growth technology of epitaxial materials. The growth of GaN on Si substrates also relies on the growth technology of lattice-mismatched materials. Deposition of polymer on Si substrate is a simple way, but the polymer cannot endure high-temperature process and so possibly limits its compatibility with current IC technology. In the above approaches, either the Si material is significantly modified or other material is used for light emission, so the original conduction-band minimum and valence-

*Correspondence: Email: cflin@cc.ee.ntu.edu.tw; Telephone: 886-2-23635251 ext. 339; Fax: 886-2-23638247

band maximum of Si is not used for radiative recombination, leading to the light emission shifting away from the Si bandgap energy. Those modifications are mostly complicated or incompatible with current Si-based IC technology.

1.2. Our Approach

In this work, we propose a new way for electroluminescence from Si without significantly modifying the Si material property. The electroluminescence is based on the metal-oxide-semiconductor (MOS) structures on Si. The oxide is grown by the well-controlled rapid thermal oxidation (RTO). The emission corresponds to bandgap energy and longer wavelengths. Their physical reasons will be discussed. Such MOS structures with the RTO grown oxide are particularly advantageous over other types of luminescence on Si because their processing steps are completely compatible with the IC fabrication. MOS on both p-type and n-type Si exhibits the electroluminescence, so it could be directly integrated with the popular CMOS technology.

Conventional MOS structures are used in field-effect transistors for isolating the gate contact from the conducting channels. It is important to have good insulation property in the oxide so that no current flows through the oxide. In our case, in order to have electroluminescence, significant current has to flow through the oxide. This could be achieved by two ways. First, the oxide layer contains lots of defects or ions. Second, the oxide is so thin that significant carriers could tunnel through quantum mechanically. The first one had been investigated recently using Ag/SiO_2/Si structure or similar MOS structures with native oxide.[22, 23] Visible electroluminescence (EL) had been reported from such structures. However, the native oxide usually contains deficient defects and its property strongly relies on the forming environment. [24] As a matter of fact, the luminescence is due to luminescent centers or oxygen deficient defects in the native oxide. In this work, we adapt the second approach. The oxide is grown by well-controlled RTO and is only a few nanometers to allow tunneling current. The high-temperature process of RTO makes the grown oxide very stable and immune to environmental variations after the growth.

2. SAMPLE PREPARATION

2.1. Oxide Growth

The MOS structures used in the study were grown on (100) Si wafers. Both n-type and p-type wafers had been used. The resistivity of the 100 mm n-type and p-type wafers is 1-10 ohm-cm and 1-5 ohm-cm, respectively. The gas flows in RTO are 500 sccm nitrogen and 500 sccm oxygen. Ultra pure gases were used in the growth chamber to eliminate possible formation of undesired ions in the oxide. Several samples had been grown by RTO. The first one has 2.3 nm oxide grown on the p-type Si wafer. The second one has 3.3 nm oxide grown on the n-type Si wafer. Their growth conditions are both at the pressure of 500 mbar and temperature of 900 °C. The thickness was measured by ellipsometry and confirmed by x-ray reflectivity. The third one has the oxide grown on the p-type wafer and the forth one has the oxide grown on the n-type wafer. Their growth conditions are changed to under reduced pressure and at temperature of over 1000 °C. The oxide also has the thickness around 3 nm.

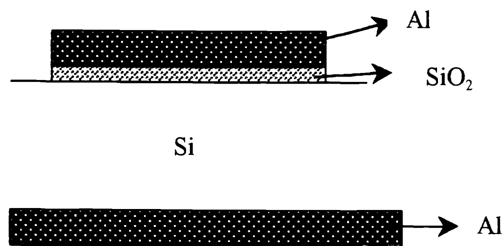

Fig. 1 A schematic of MOS strucutres

2.2. Metalization

The Aluminum metal was then deposited on top of the oxide by evaporation right after RTO in order to prevent the regrowth of native oxide as a result of the exposure to atmosphere. After the deposition of the Al on the oxide, another metalization for ohmic contact was performed on the other side of the Si wafer. Then on the oxide side, patterns with circular areas and straight lines of Al pads were formed by chemical etching. The circular areas have diameters of 2.5 mm, 1mm, and 0.5mm. The straight lines are of width 0.1 mm. The device structures are schematically shown in Fig. 1. Measurements were done by applying the voltage across the Si side and the metal on top of the oxide.

3. EXPERIMENTAL RESULTS

3.1 Electrical characteristics

Fig. 2 shows a typical cw J-V curve of the MOS on n-type Si without cooling. This curve was measured on the device with 2mm-diameter Al pads. The voltage was applied between the metal on top of oxide and Si. This curve shows fair rectification characteristics. For the MOS on n-type Si, significant current could flow through the oxide when this metal is positively biased. On the other hand, significant current is measured when the metal on top of oxide is negatively biased for the MOS on p-type Si. Adapting the terminology of conventional diodes, we name this condition with large current flow as forward bias and the opposite bias as reversed bias. The MOS on p-type Si has a similar J-V curve except that its turn-on voltage is larger because the Al Fermi-level (E_{fm}) is closer to the valence band of Si than the conduction band.

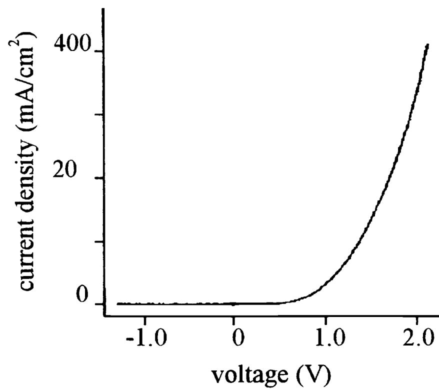

Fig. 2 A typical J-V curve for MOS with thin oxide on n-type silicon.

The low-temperature J-V curve was also measured. As shown in Fig. 3, the temperature does not have strong influences on the J-V characteristics, indicating that the current flow is mainly caused by the tunneling effect.

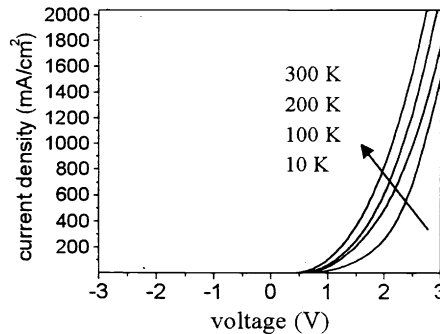

Fig. 3 J-V curves for MOS with thin oxide at different temperatures.

3.2. Electroluminescence

Under the forward bias, the two samples with oxide grown at the pressure of 500 mbar exhibited luminescence that could be clearly observed through an IR-viewer. The emission mainly emitted from the periphery of the circular area because the metal pads were made of thick aluminum. Therefore, only a small portion of light was measured. The shape is like the total eclipse of sun. The eclipse-like luminescence could be clearly observed through the IR-viewer even with a current density as low as 0.67 A/cm^2. Under the reversed bias, no luminescence was observed.

3.2.1 L-I Characteristics

Fig. 4 shows the measured L-I curve (output power vs. injection current) for the MOS structures on n-type Si under cw operation without cooling under the low applied voltage. As the applied voltage increases, the L-I curve behaves differently, as shown in Fig. 5. This curve is measured for the MOS on p-type Si. The L-I curve consists of two different parts, regions I and II. They correspond to the applied voltage approximately below and above 5 V, respectively. For region I, the curve shows a superlinear increase of the output power with the injection current. In region II, abnormal L-I characteristics are observed. The MOS on n-type Si has similar behaviors except that region II occurs for the applied voltage approximately above 10 V. The reason can be explained as follows. Because the MOS on n-type Si has a larger current under the same bias, most of the voltage drops across the thick Si substrate instead of the oxide. As a result, the applied voltage appears to be larger.

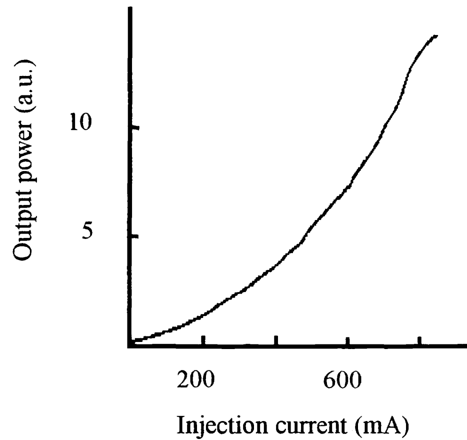

Fig. 4 The L-I curve of the electroluminescence from the MOS on n-type Si under low applied voltage.

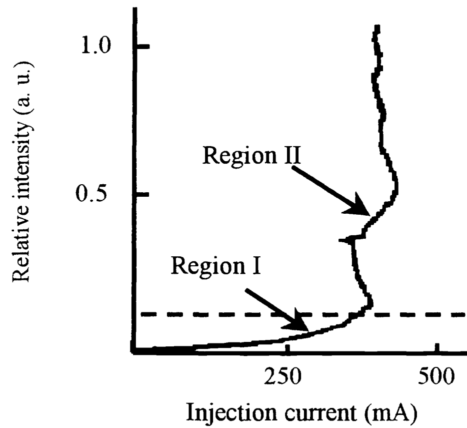

Fig. 5 The L-I characteristics of the electroluminescence from the MOS on p-type silicon.
Region I: below dash line; region II: above dash line.

3.2.2 Emission Spectra

The emission spectra were measured using a monochromator from the circular area of 2.5 mm-diameter Al pad on top of oxide. Figs. 6 (a) and (b) show the measured spectra with the emission centered around 1150 nm and 1180 nm for the MOS on p-type and n-type Si, respectively, under cw operation without cooling. Both correspond to the bandgap energy Eg of Si slightly above the room temperature. Because the MOS on n-type Si has a larger current than the MOS on p-type Si under the same bias, more ohmic heat is generated, leading to the longer wavelength for the MOS on n-type Si. These spectra correspond to Region I of the L-I curve in Fig. 5. Only the two samples with oxide grown at the pressure of 500

mbar exhibited the emission at bandgap energy. The other two samples with oxide grown at reduced pressure shows no emission at this wavelength at all.

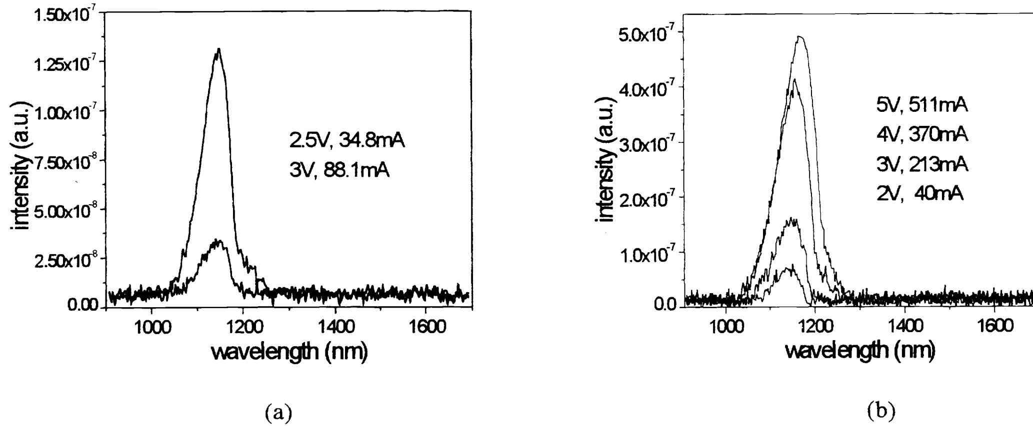

Fig. 6 The measured spectra under cw operation without cooling from the MOS on (a) p-type Si (b) n-type Si.

By increasing the applied voltage, the emission power initially increases with the injection current, but then gradually decreases as the voltage approaches 5 V or 10 V for MOS on p-type Si or n-type Si, respectively. When the applied voltage increases beyond 5 V or 10 V, the luminescence near 1150 nm completely vanishes and then luminescence at longer wavelengths appears. The measured spectra are shown in Fig. 7 at different applied voltages for the MOS on p-type Si. These spectra correspond to the abnormal characteristics of region II of the L-I curve in Fig. 5. As shown in Fig. 7, when the applied voltage further increases, the spectra move toward shorter wavelengths, but are still longer than 1200 nm. The measured spectral range is limited by the InGaAs detector. The entire spectra should extend beyond 1700 nm. All of the four samples exhibited such voltage-dependent emission beyond 1200 nm.

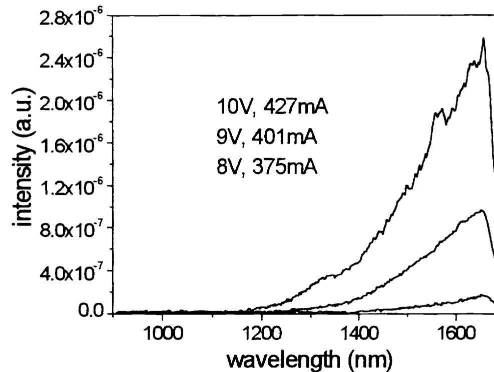

Fig. 7 The measured spectra under cw operation without cooling for region II in Fig. 5.

3.2.3 Discussion on Emission Spectra

Different from other reports, [22, 23, 25] our devices exhibit no visible luminescence. The previously reported visible luminescence from the MOS with native oxide [25, 26] is probably due to luminescent centers or oxygen deficient defects in the native oxide. In our devices, because the oxide was grown by the well-controlled RTO, it should have much less defects than the native oxide. Thus visible luminescence is not observed. The C-V measurements further confirm that there is negligible interface trap in the oxide or near the interface of the oxide and Si. The different luminescence in our devices

should be due to different mechanisms involved. The mechanisms for the emissions near bandgap energy and longer wavelengths will be discussed separately in the following.

4. THEORETICAL EXPLANATION

4.1. Emission at Bandgap Energy

The discussion for the emission around Eg is based on the MOS on p-type Si only because the physical reason for the MOS on n-type Si is similar. A schematic of the band diagram shown in Fig. 8 is used for the explanation. For the MOS on p-type Si, E_{fm} increases with the forward bias. Electrons then tunnel from metal to Si and holes tunnel vice versa. The major contribution of current comes from the tunneling of electrons instead of holes for the MOS on p-type Si. [27] Increasing the negative bias at the metal side causes E_{fm} to shift up to the conduction band edge (Ec). Then the tunneling current significantly increases because the tunneling electrons could fill in many states in the conduction band. On the other hand, the negative bias of metal causes the band of the p-type silicon to bend up near the Si/SiO_2 interface, as schematically shown in Fig. 8. A potential well for hole confinement is then formed, leading to the accumulation of holes near the interface. Consequently, huge population of the holes and the tunneling electrons simultaneously appear in the well region.

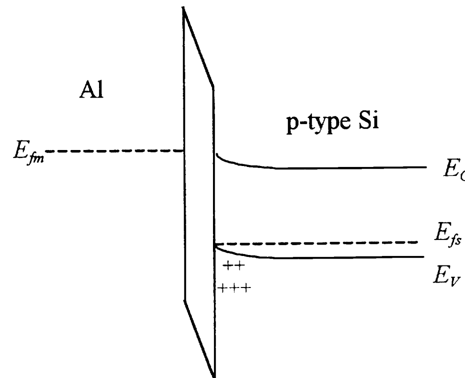

Fig. 8 A schematic of the band diagram with the metal of the MOS on p-type Si negatively biased.

In addition to the simultaneous appearance of many electrons and holes in the same region, momentum conservation is also necessary to have radiative recombination. This could not, in general, happen in the indirect-bandgap material. However, if there is any lattice disorder near the Si/SiO_2 interface, [28] the requirement of momentum conservation could be relaxed. In the formation of oxidation during RTO, small-scale roughness at the interface could be possibly formed to provide extra momentum required for radiative recombination for electrons and holes.

Because the Si atoms on the top surface of the (100) Si wafer have their atom spacing less than the total bonding length of Si-O-Si, not each atom could be chemically bonded with oxygen atoms. Then some Si atoms are not oxidized. Those atoms are named as s-Si for simple explanation later. Similarly, the others that are chemically bonded with oxygen atoms are named as o-Si. Because the s-Si atoms on the top surface are not oxidized, they are still part of the semiconductor. On the other hand, they are closer to metal than other Si atoms in the semiconductor below the top layer, so more electrons tunnel to the region of s-Si atoms. Therefore, many tunneling electrons are localized around the s-Si atom in the direction parallel to the interface, causing their wavefunction to be laterally localized. Then their wavefunction in the momentum space will have a large spread in the corresponding direction according to the uncertainty principle. The extra momentum required for the electron-hole radiative recombination is thus provided.

In the extreme case, each s-Si atom on the top surface is surrounded by o-Si atoms, so the lateral localization is in the range less than the lattice constant. As a result, the electron tunneling to s-Si atom has a spatial wavefunction localized to within the lattice constant a. Its Fourier-transformed wavefunction in k-space could then extend to beyond $2\pi / a$, which is sufficient to compensate for conduction-band minimum near the X point. Therefore, electron-hole radiative recombination is largely enhanced.

Those samples with the thin oxide grown by RTO at the reduced pressure had also been measured. Because of the thin oxide, significant current was still obtained when they were forward biased. The reduced pressure causes Si atoms on

the top surface of Si wafer to be less oxidized. As a result, more s-Si atoms are neighboring together instead of being laterally isolated by o-Si atoms. Because the corresponding spatial wavefunction of tunneling electrons is less confined, the wavefucntion in k-space has less spread, leading to insufficient momentum for the compensation. Therefore, those samples exhibit no emission corresponding to Si bandgap energy although they also demonstrate behaviors of diodes. They also have no visible luminescence, indicating that the oxide grown at reduced pressure contains negligible defects to work as luminescent centers.

The emission energy corresponding to 1150 nm and 1180 nm is slightly less than Si bandgap energy at the room temperature. They could be explained by the following reasons. First, the increasing carrier density [29] might result in the bandgap shrinkage and so the red shift. Second, the interruption of Si periodical structure at the interface causes band bending and the bandgap shrinkage. [30] Third, the large injection current leads to significant ohmic heat and temperature rise, so the bandgap energy is reduced. The ohmic heat could also explain the MOS on n-type Si emitting light at a longer wavelength because it has a larger current under the same bias.

4.2. Emission at Wavelengths Longer Than 1200 nm

When the applied voltage increases to be much larger than the Fermi-level difference, E_{fm} moves far above Ec, as schematically shown in Fig. 9. The electrons with energy E_1 near Ec then see an increased potential barrier, so their tunneling probability is reduced. On the other hand, the electrons with their energy E_2 near E_{fm} have increased tunneling probability as a result of the strongly tilted potential barrier. Those electrons tunnel into the high-energy states of the conduction band. Therefore, radiative recombination corresponding to Eg is reduced. The emission corresponding to the bandgap energy therefore disappears, as shown in Fig 7.

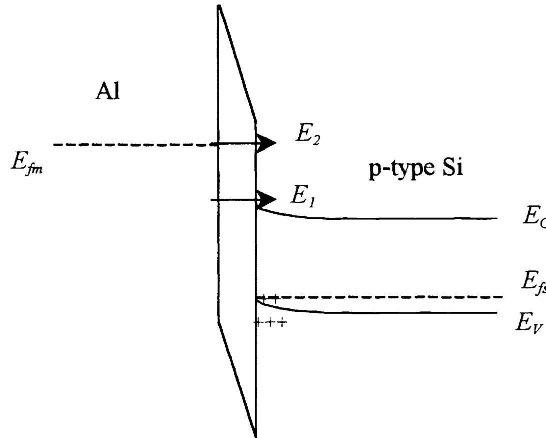

Fig. 9 A schematic of the band diagram with the metal of the MOS structure negatively biased for E_{fm} far above Ec.

Fig. 7 also shows that the emission shifts to longer wavelengths at large applied voltages. This emission was observed for all of the four samples described in Section II. The reasons for such emission are discussed as follows. First, it might be possibly due to the interfacial states in the grown oxide. However, the C-V measurement indicates only very small amount of interface trap in the oxide, implying that the interfacial states are probably not significant. In addition, the spectrum is voltage-dependent, so the interfacial states should not be the main cause. Second, black-body radiation might also be the reason. To identify if the emission is caused by black-body radiation, similar measurements had been done with the sample cooled. Under the same bias condition, the emission near 1600 nm for the sample cooled down to 10 K is even stronger than at 300 K, indicating that black-body radiation alone could not explain the emission well. Third, as E_{fm} moves up further, as shown in Fig. 9, electrons tunnel to the states far above Ec. Those hot carriers could then relax to lower energy states, e.g. $E_2 \rightarrow E_1$, by direct or phonon-assisted inter-conduction-band radiation. [31, 32] A gradual shift of spectrum from 1200 nm to beyond 1300 nm with increasing applied voltages for MOS on n-type Si had been observed, indicating the possibility of the third mechanism. As discussed before, at large applied voltages, the number of tunneled carriers with energy near band edge is reduced, while more carriers tunnel into the high-energy states. Therefore, emission corresponding to Eg is reduced and probability of direct or phonon-assisted c-c or v-v radiation increases.

Although the above discussion is for the MOS on p-type Si, the physics of the MOS on n-type Si are similar. The only difference is that the major role becomes the hole instead of the electron.

Different from the physics involved in the emission at bandgap energy, the emission at longer wavelengths is not due to the surface roughness. Therefore, all of the four samples should exhibit the emission characteristics regardless of the growth pressure, as demonstrated experimentally.

5. CONCLUSION

In conclusion, room-temperature electroluminescence from the simple MOS structure on silicon is observed. The thin oxide grown by the well-controlled RTO provides the mechanism for carrier tunneling quantum mechanically. The MOS then behaves like light emitting diodes. Under low applied voltages, the emission wavelength is around 1150 nm, which approximately corresponds to Si bandgap energy. This emission is attributed to the roughness generated at the Si/SiO_2 interface during RTO. This roughness accounts for the compensation of extra momentum required in radiative recombination in indirect-bandgap materials. When the applied voltage is increased to much larger than the Fermi-level difference between the metal and Si, the emission wavelength becomes longer than 1150 nm and voltage-dependent. The emission is possibly caused by direct or phonon-assisted c-c or v-v radiative transition.

ACKNOWLEDGEMENTS

This work is supported in part by National Science Council, Taipei, Taiwan, R.O.C. under the contract No. 88-2218-E-002-004, No. NSC88-2215-E-002-021, and No. NSC2112-M-002-038.

REFERENCES

1. N. Takato, K. Jinguji, M. Yasu, H. Toba, and M. Kawachi, *IEEE J. Lightwave Technol.* **6**, pp. 1003-1010, 1988.
2. G. V. Treyz, P.G. May, and J.-M. Halbout, *Appl. Phys. Lett.* **59**, pp. 771-773, 1991.
3. M. L. Cohen and T. L. Bergstresser, *Phys. Rev.* **141**, pp. 789-796, 1966.
4. M. C. Wu, L.-Y. Lin, S.-S. Lee, and K. S. J. Pister, *Sensors and Actuators* **A 50**, pp. 127-134, 1995.
5. L. T. Canham, *Appl. Phys. Lett.* **57**, pp. 1046-1048, 1990.
6. N. Koshida and H. Koyama, *Appl. Phys. Lett.* **60**, pp. 347-349, 1992.
7. S. Lazarouk, P. Jaguiro, S. Katsouba, G. Masini, S. La Monica, G. Maiello, and F. Ferrari, *Appl. Phys. Lett.* **68**, pp. 2108-2110, 1996.
8. H. Ennen, J. Schneider, G. Pomerenke, A. Axmann, *Appl. Phys. Lett.* **43**, pp. 943-945, 1983.
9. G. Franzo, F. Priolo, S. Coffa, A. Polman, and A. Carnera, *Appl. Phys. Lett.* **64**, pp. 2235-2237, 1994.
10. M. Matsuoka, and S. Tohno, *Appl. Phys. Lett.* **71**, pp. 96-98, 1997.
11. L. S. Liao, X.-M. Bao, X.-Q. Zheng, N.-S. Li, and N.-B. Min, *Appl. Phys. Lett.* **68**, pp. 850-852, 1996.
12. W. Skorupa, R. A. Yankov, I. E. Tyschenko, H. Frob, T. Bohme, and K. Leo, *Appl. Phys. Lett.* **68**, pp. 2410-2412, 1996.
13. S. Oguz et al., *Appl. Phys. Lett.* **43**, pp. 848-850, 1983.
14. C. W. Liu, J. C. Sturm, Y. R. J. Lacroix, M. L. W. Thewalt, and D. D. Ferovic, *Mat. Res. Soc. Symp. Proc.* **342**, pp. 37-42, 1994.
15. S. Schuppler, S. L. Friedman, M. A. Marcus, D. L. Adler, Y.-H. Xie, F. M. Ross, Y. J. Chabal, T. D. Harris, L. E. Brus, W. L. Brown, E. E. Chaban, P. F. Szajowski, S. B. Christman, and P. H. Citrin, *Phys. Rev.* **B 52**, pp. 4910-4925, 1995.
16. D. B. Geohegan, A. A. Puretzky, G. Duscher, and S. J. Pennycook, *Appl. Phys. Lett.* **73**, pp. 438-439, 1998.
17. F. Buda et al., *Phys. Rev. Lett.* **69**, pp. 1272-1275, 1992.
18. D. R. Baigent, R. N. Marks, N. C. Greenham, R. H. Friend, S. C. Moratti, and A. B. Holmes, *Appl. Phys. Lett.* **65**, pp. 2636-2638, 1994.
19. R. Birkhahn and A. J. Steckl, *Appl. Phys. Lett.* **73**, pp. 1700-1702, 1998.
20. M. Garter, J. Scofield, R. Birkhahn, and A. J. Steckl, *Appl. Phys. Lett.* **74**, pp. 182-184, 1999.
21. Zhanghua Wu, Tomonobu Nakayama, Shan Qiao, and Masakazu Aono, *Appl.Phys. Lett.* **74**, pp. 3842-3844, 1999.
22. Y. Q. Wang, T. P. Zhao, J. Liu and G. G. Qin, *Appl. Phys. Lett.*, **74**, pp. 3815-3817, 1999.
23. J.Yuan and D. Haneman, *J. Appl. Phys.* **86**, pp. 2358-2360, 1999.
24. *ULSI technology*, edited by Chang, C. Y. and Sze, S. M., New York, McGraw-Hill, 1996.
25. G. F. Bai, Y. Q. Wang, Z. C. Ma, W. H. Zong, and G. G. Qin, *J. Phys.: Condens. Matter* **10**, L717-L721, 1998.
26. D. L. Griscom, *J. Ceram. Soc. Jpn.* **99**, 899, 1991.

27. C. W. Liu, M. H. Lee, C. F. Lin, I. C. Lin, W. T. Liu, and H. H. Lin, *1999 IEEE International Electron Devices Meeting*, Paper 31.3, Washington, D. C., December, 1999.
28. M. Jaros and A. W. Beavis, *Appl. Phys. Lett.* **63**, pp. 669-671, 1993.
29. H. C. Casey, Jr. and M. B. Panish, *Heterostructure Lasers*, Part A, Academic Press, Orlando, 1978.
30. S. M. Sze, *Physics of Semiconductor Devices*, 1981.
31. J. Bude, N. Sano, and A. Yoshii, *Phys. Rev.* **B 45**, pp. 5848-5856, 1992.
32. L. Carbone, R. Brunetti, C. Jacoboni, A. Lacaita, and M. Fischetti, *Semicond. Sci. Technol.* **9**, pp. 674-676, 1994.